Biomaterials 33 (2012) 4576–4588

Contents lists available at SciVerse ScienceDirect

Biomaterials

journal homepage: www.elsevier.com/locate/biomaterials

The accumulation of dual pH and temperature responsive micelles in tumors

Yi-Chun Chen [a], Li-Chi Liao [a], Pei-Lin Lu [b], Chun-Liang Lo [c], Hsieh-Chih Tsai [d], Chiung-Yin Huang [e], Kuo-Chen Wei [e], Tzu-Chen Yen [f], Ging-Ho Hsiue [a,b,*]

[a] Department of Chemical Engineering, National Tsing Hua University, Hsinchu 300, Taiwan, ROC
[b] R&D Center for Membrane Technology, Chung Yuan Christian University, Chungli 320, Taiwan, ROC
[c] Department of Biomedical Engineering, National Yang Ming University, Taipei 112, Taiwan, ROC
[d] Graduate Institute of Applied Science and Technology, National Taiwan University of Science and Technology, Taipei 106, Taiwan, ROC
[e] Department of Neurosurgery, Chang Gung University College of Medicine and Memorial Hospital, Taoyuan 333, Taiwan, ROC
[f] Department of Nuclear Medicine and Molecular Imaging Center, Chang Gung Memorial Hospital, Taoyuan 333, Taiwan, ROC

ARTICLE INFO

Article history:
Received 2 January 2012
Accepted 14 February 2012
Available online 23 March 2012

Keywords:
Polymeric micelles
Temperature-responsive
pH-responsive
EPR effect
Doxorubicin

ABSTRACT

An optimized, biodegradable, dual temperature- and pH-responsive micelle system conjugated with functional group Cy5.5 was prepared in order to enhance tumor accumulation. The Dynamic light scattering (DLS) measurements showed that these diblock copolymers form micelle in PBS buffer with a size of around 50 nm by heating of an aqueous polymer solution from below to above the cloud point (CP). Anticancer drug, doxorubicin was incorporated into the inner core of micelle by hot shock protocol. The size and stability of the micelle were controlled by the copolymer composition and is fine tuned to extracellular pH of tumor. The mechanism then caused pH change and at body temperature which induce doxorubicin release from micelles and have strong effects on the viability of HeLa, ZR-75-1, MCF-7 and H661 cancer cells. Our *in vivo* results revealed a clear distribution of Doxorubicin-loaded mixed micelle (Dox-micelle) and efficiency targeting tumor site with particles increasing size in the tumor interstitial space, and the particles could not diffuse throughout the tumor matrix. *In vivo* tumor growth inhibition showed that Dox-micelle exhibited excellent antitumor activity and a high rate of anticancer drug in cancer cells by this strategy.

1. Introduction

Technical advances have enabled the preparation of anticancer particles with greater specificity and fewer side effects [1–3]. Tumors have aberration of tumor blood and lymphatic vasculature, which provides access to circulating particles [4,5]. For specific targeting efficiency, studies have phenomenally selective targeting of designed nanostructures to tumor within this size range (10–100 nm) accumulate within solid tumors owing to the enhanced permeability and retention effect (EPR effect) [6,7]. The effect began a development of nanometer-sized carriers to more efficiently deliver therapeutic and/or diagnostic agents [7–11]. Various *in vivo* investigations have demonstrated that nanoparticle size is a key determinant to target tumor site [9–11]. Perrault *et al.* examined the permeation of nanoparticles within the tumor is highly dependent on the overall size of the pegylated gold nanoparticles, where larger nanoparticles (100 nm) appear to stay near the vasculature of tumor while smaller nanoparticles (20 and 60 nm) rapidly diffuse throughout the tumor matrix [11]. To reduce side effects, carriers can be designed to respond to stimuli tumor sites (e.g., increases in local temperature [12] or decreases in extracellular pH [13]), and nanoparticles responsive to both temperature and pH (e.g., constructed from poly(*N*-isopropylacrylamide) and a pH-sensitive copolymer) [14–16] can distinguish between normal and pathological tissues. These particles are temperature-sensitive because the poly(*N*-isopropylacrylamide) precipitates above the cloud point (CP) of ~32 °C [17]. However, such particles have limited applicability because drugs can be released by hypothermia. Also, these dual responsive particles have a strong negative surface charge [15,16], making them susceptible to uptake by the liver's non-parenchymal cells *via* receptor-mediated endocytosis [18].

The strategy for enhancing tumor specificity is to design the dual-responsive drug carrier and expect to accumulate in the tumor site by controllable particle size increasing. We established a multifunctional mixed micelles system using mPEG-*b*-P(HPMA-Lac-*co*-His) (Scheme 1) with dual-responsive diblock copolymer and mPEG-*b*-PLA with low critical micelles concentration (CMC) value diblock copolymer (schematic representation in Fig. 1a). The

* Corresponding author. Department of Chemical Engineering, National Tsing Hua University, Hsinchu 300, Taiwan, ROC. Tel.: +886 3 571 9956; fax: +886 3 572 6825.
E-mail address: ghhsiue@mx.nthu.edu.tw (G.-H. Hsiue).

0142-9612/$ – see front matter © 2012 Elsevier Ltd. All rights reserved.
doi:10.1016/j.biomaterials.2012.02.059

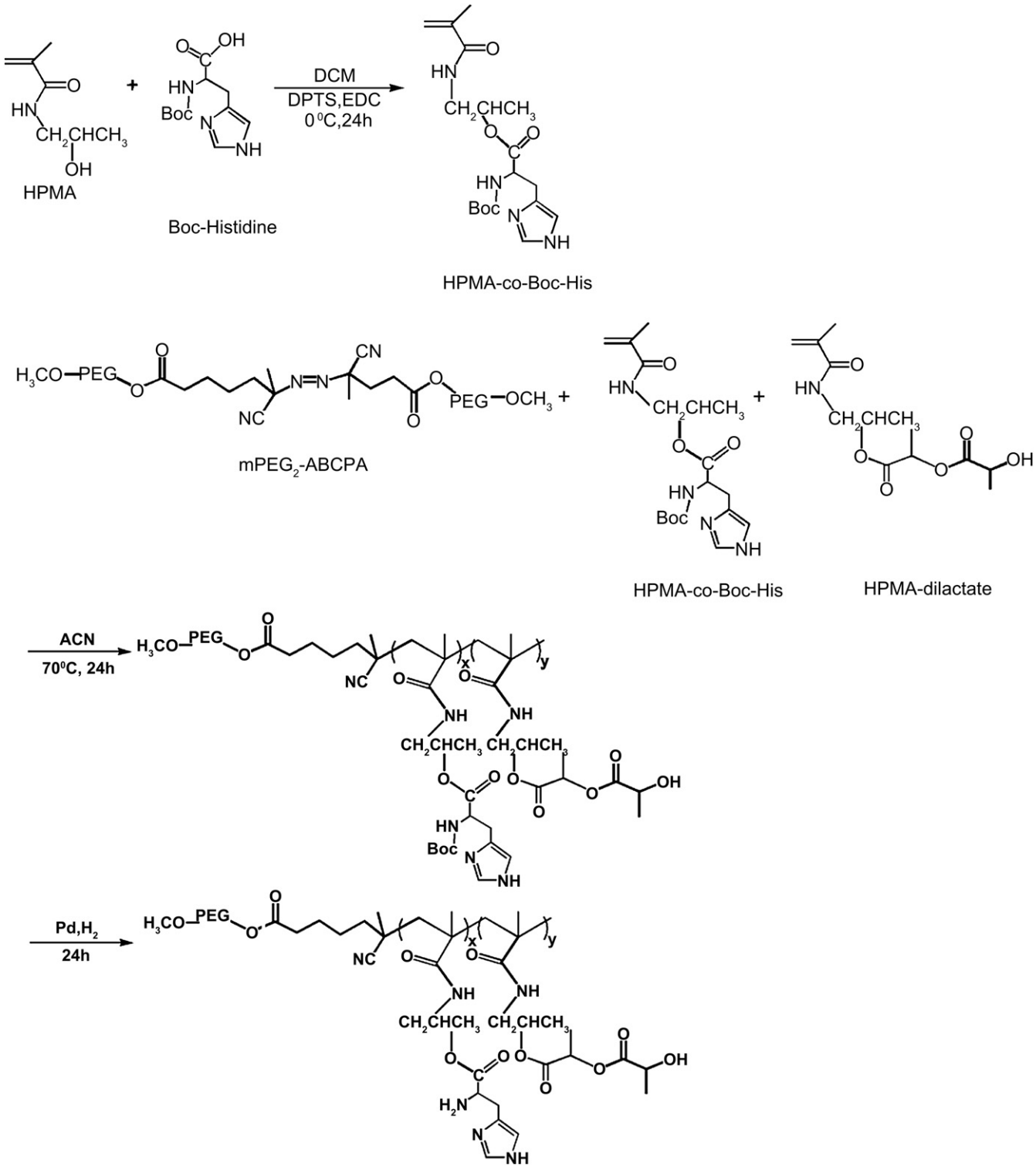

Scheme 1. Chemical synthesis route of mPEG-b-P(HPMA-Lac-co-His).

hydrophobic segment of dual-responsive copolymer was composed of poly(N-(2-hydroxypropyl) methacrylamide dilactate)-*co*-(N-(2-hydroxypropyl) methacrylamide-*co*-histidine). Poly(*N*-(2-hydroxypropyl) methacrylamide dilactate) has a thermoreversible LCST suitable for the targeted delivery of paclitaxel, photosensitizers and superparamagnetic iron oxide [19–21] because hydrophobic lactate side chains are hydrolyzed at physiological temperature [22–24]. Histidine is useful in pH-sensitive polymeric drug delivery systems because of its buffering capacity ($pK_b = \sim 6.02$) and because its imidazole ring has a lone pair of electrons on an unsaturated nitrogen (NH of pyrrole) [25,26]. In contrast, PEG acts as a highly hydrophilic block that offers stability to the drug carrier, as well as allowing the micelles to avoid recognition by monocytes [27,28]. The products after micelles

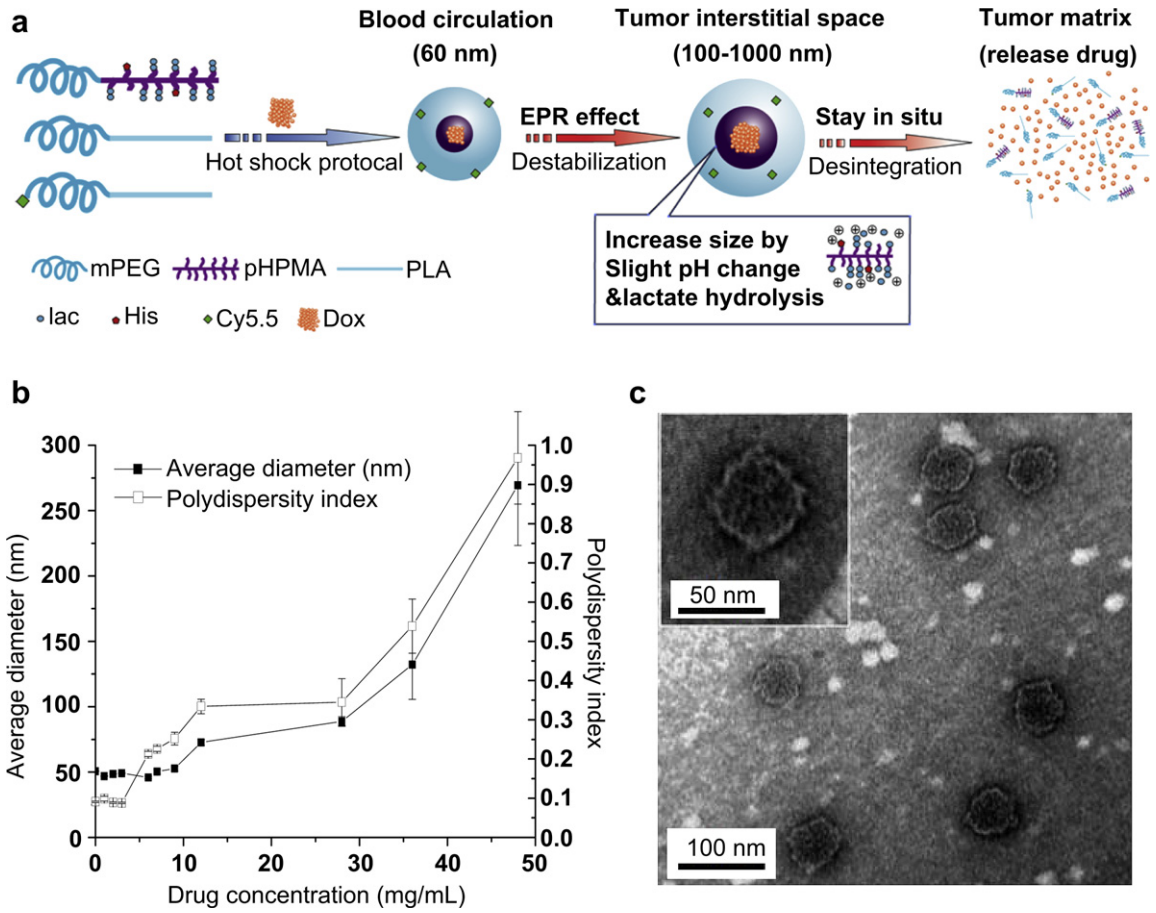

Fig. 1. (a) Schematic representation of mixed micelle composed of the diblock copolymers mPEG-*b*-P(HPMA-Lac-*co*-His), mPEG-*b*-PLA and Cy5.5-PEG-PLA and loaded with doxorubicin. The dual-responsive drug carrier is designed with stealth behavior in blood circulation. Micelle permeated through tumor interstitial space and maintained accumulation in tumor matrix. Finally, dual responsive micelle disintegrated and release the anticancer drug rapidly in tumor matrix. (b) Evaluation of the change in micelle size and polydispersity index of Dox-micelle in PBS solution (pH 7.4) at 37 °C, as determined by dynamic light scattering. Mean ± SD ($n = 3$). (c) Transmission electron micrographs of Dox-micelle at 1 h and in PBS (pH 7.4).

degradation, such as lactic acid, histidine, HPMA and mPEG are non-cytotoxic. Most importantly, the biodegradable dual responsive micelles could restrict particle diffusion throughout the tumor matrix by the controllable particle size. Linking the cyanine dye Cy5.5 to the end of mPEG-*b*-PLA permits the distribution of the micelles to be monitored for *in vitro* and *in vivo* by fluorescence microscopy.

2. Materials and methods

2.1. Materials

Methoxy poly(ethylene glycol) with Mw 5000 (mPEG), α-t-butyloxy-carbonylamino-ω-hydroxy-poly(ethylene glycol) (Boc–NH–PEG-OH) with Mw 3000 was purchased from Iris Biotech. D,L-lactide and palladium were purchased from Lancaster. Cy5.5 mono NHS ester was purchased from GE Healthcare. N-(2-hydroxypropyl) methacrylamide (HPMA) were purchased from Polysciences. 4,4′-Azobis(4-cyanovaleric acid) (ABCPA) and stannous octoate ($Sn(Oct)_2$ were purchased from Aldrich. Sodium hydroxide (NaOH), bovine serum albumin (BSA), potassium chloride (KCl), potassium hydrogen phosphate (KH_2PO_4), sodium chloride (NaCl) and disodium hydrogen phosphate (Na_2HPO_4) were purchased from Sigma. Dimethyl sulfoxide (DMSO), 4-(dimethylamino)pyridine (DMAP), N-(tert-butoxycarbonyl)-L-histidine and 1-(3-dimethylaminopropyl)-3-ethylcarbodiimide (EDC) were purchased from TCI. Acetonitrile (ACN), diethyl ether, dichloromethane (DCM) and ethanol (EtOH) were purchased from TEDIA. LysoSensor™ Blue DND-167 was purchased from Molecular Probes. Dulbecco's modified Eagle's medium (DMEM), RPMI-1640 medium and penicillin-streptomycin were purchased from GIBCO. Fetal bovine serum (FBS) was purchased from Invitrogen. All cell lines were obtained from the Bioresource Collection and Research Center, Hsinchu, Taiwan.

2.2. Synthesis of mPEG-b-PLA, NH_2-PEG-PLA and Cy5.5-PEG-PLA

mPEG-*b*-PLA diblock copolymer was synthesized by ring-opening polymerization [25,29,30]. mPEG with Mw 5000 and toluene were added to a two-necked round-bottle flask with a magnetic stirrer. Stannous octoate was then added to start the polymerization at 130 °C for 16 h under nitrogen. After polymerization the reaction was terminated by adding 0.1 N methanolic KOH and the product recrystallized from diethyl ether at 0 °C. Boc–NH–PEG-PLA diblock copolymer was also synthesized by ring-opening polymerization [26,30]. D,L-lactide, Boc–NH–PEG (Mw 4750, 3000) and toluene were added to a two-necked round-bottle flask with magnetic stirrer. Stannous octoate was then added to start the polymerization, which was carried out at 130 °C for 16 h under nitrogen. After polymerization, the reaction was terminated by adding 0.1 N methanolic KOH and the product recrystallized from dichloromethane and diethyl ether co-solvent. The Boc–NH–PEG-PLA was then reacted with H_2 in the presence of Pd catalyst at room temperature for 24 h to remove Boc. The final product was obtained after filtering out the Pd catalyst and precipitating from diethyl ether. Micellar shells were constructed from the functional copolymer Cy5.5-PEG-PLA by dissolving Cy5.5 NHS ester and NH_2-PEG-PLA in DMSO for 16 h at room temperature, dialyzing (MW cutoff 2000 Da) against deionized water for 24 h, and freeze-drying. The resulting Cy5.5-PEG-PLA copolymers [26,30] were stored in the dark at 4 °C until use; quantitative analysis of Cy5.5 conjugation to PEG-PLA was determined by measuring fluorescence intensity. Micelles with Cy5.5-PEG-PLA can be monitored real-time near-infrared (NIR) fluorescence intensity in the whole body. mPEG-PLA and Cy5.5-PEG-PLA of weight-average molecular weight and polydispersity index (PDI) were 6290/5930 and 1.15/1.13, respectively.

2.3. Synthesis of mPEG-b-P(HPMA-Lac-co-His)

To introduce pH-sensitive moieties into the hydrophobic segment, the monomer HPMA-*co*-Boc-His was obtained by esterification using the hydroxyl group of HPMA as the ethanol and the carboxyl group of Boc-histidine as the acid. Boc-histidine

(1 mmol), HPMA (1 mmol), and dimethylamino pyridinium toluene sulfonic acid (DPTS; 0.3 mol) were dissolved in dichloromethane (DCM). EDC (1-ethyl-3-(3-dimethylaminopropyl)carbodiimide; 1.5 mmol) was dissolved in DCM and added dropwise to the mixture. The reaction was carried out for 24 h at 0 °C in an ice bath. The NMR and mass spectrums were shown as Figs. S1 and S2 in the Supporting Information. Finally, to synthesize mPEG-*b*-P(HPMA-Lac-*co*-His) diblock copolymers (Scheme 1), HPMA-dilactate [22,23], HPMA-*co*-Boc-His, and $mPEG_2$-ABCPA macroinitiator [29] were dissolved in ACN. After purging with N_2, the reaction was conducted at 70 °C for 24 h under nitrogen. The products were precipitated with diethyl ether and collected by centrifugation. Then the copolymer was dissolved in ethanol in the presence of Pd catalyst and reacted with hydrogen at room temperature for 24 h. The polymers were purified by dissolving them in cold water, followed by filtration through a 0.22 μm filter and freeze-drying. Also, to synthesize mPEG-*b*-P(HPMA-Lac) diblock copolymers as a reference sample [23], HPMA-dilactate and mPEG2-ABCPA macroinitiator were materials by the same protocol. mPEG-*b*-P(HPMA-Lac) had a composition of 0.7% PEG, 33.1% HPMA and 66.2% Lac with weight average, number-average molecular weight and PDI of 22325, 18604 and 1.20.

2.4. Characterizations of diblock copolymers

To modulate the phase transition temperature, the optical transmittances of the copolymers were measured at 542 nm using a UV–Vis spectrometer (PerkinElmer Lambda 2S) equipped with a temperature-controlled sample cell and a ramp speed of 1 °C/min; the CP values of 10 mg/mL copolymers in phosphate-buffered saline (PBS; pH 7.4) were determined at temperatures showing an optical transmittance of 60%. The temperature-sensitivity of diblock copolymers was also measured by dynamic light scattering and UV–Vis spectrometer. mPEG-*b*-P(HPMA-Lac), mPEG-*b*-P(HPMA-Lac-*co*-His) and mPEG-*b*-P(HPMA-Lac-*co*-His)/mPEG-*b*-PLA (75:25 wt%) was dissolved in 2 ml of pH 7.4 PBS buffer at 0 °C. The weight of copolymer or mixture was 10 mg in 2 ml solution. The particle size and PDI was directly determined by DLS (Zetasizer 3000HS, Malvern) from 10 to 45 °C. The correlation functions from DLS were analyzed by the constrained regularized CONTIN method. The CMC of the block copolymers was determined using pyrene as a fluorescent probe and obtained from a plot of the intensity ratio I_{338}/I_{333}.

2.5. Preparation of empty and Dox-loaded micelles

Dual responsive micelles were prepared by the temperature sensitive and used a modified heat shock protocol [19–21]. Micelles were formed by a quick heating of an aqueous polymer solution from below to above the CP. Different concentrations (1–10 mg/mL) of mPEG-*b*-P(HPMA-Lac-*co*-His) and mPEG-PLA were dissolved completely in PBS at 0 °C. Then the polymer solution (2 mL) was quickly heated and stirred from 0 to 60 °C and left at 60 °C for 1 min. Doxorubicin was encapsulated using the same protocol. Doxorubicin hydrochloride (20 mg, in 2 mL 99% ethanol) was mixed with 8 μL of triethylamine to remove the hydrochloride. The doxorubicin solution (0.2 mL) was added to 1–10 mL of the copolymer solution and stirred at 0 °C. The resulting mixture was heated rapidly to 60 °C while stirred for 1 min, and the ethanol was removed by rotary evaporation at 40 °C. Free doxorubicin was removed by filtration through a sterile, surfactant-free, 0.22 μm cellulose acetate filter (Sartorius Stedim). For DLS measurements, the micellar solution was incubated at 37 °C for 1 h. Dox-micelles stained with 2% uranyl acetate were examined by transmission electron microscopy to investigate their size and morphology.

2.6. Differential scanning calorimetry (DSC) measurement

DSC measurements of the lyophilizing mPEG-*b*-PLA micelles, mPEG-*b*-P(HPMA-Lac-*co*-His) micelles, mixed micelles and the mixture of mPEG-*b*-PLA/mPEG-*b*-P(HPMA-Lac-*co*-His) micelles were made using a PerkinElmer PYRIS Diamond DSC in sealed aluminium pans. A temperature range of −20–100 °C was scanned at a heating rate of 20 °C/min. The samples were cooled immediately to −20 °C, which temperature was held for 10 min, before they were heated again from −20–100 °C at a heating rate of 20 °C/min. The midpoints of the change in the heat capacity in the DSC thermal diagram obtained in the second heating run were taken as the glass transition temperature.

2.7. Drug release assay

The time course of controlled drug release from Dox-micelles (50 mg/L) at 25 and 37 °C was assessed over a range of pH values by monitoring diffusion from a cellulose membrane dialysis bag (MW cutoff of 6000–8000; SpectrumLabs, Inc.) with UV–Vis spectrometry at 485 nm.

2.8. Cytotoxicity evaluation

The cytotoxicity of each sample was determined by measuring the inhibition of cell growth using a tetrazolium dye (MTT) assay. Human cervical carcinoma (HeLa), human breast carcinoma (ZR-75-1 and MCF-7) and human lung large cell carcinoma (NCI-H661 abbreviated to H661) (5×10^3 cell mL^{-1}) harvested in the logarithmic growth phase were seeded on 96 wells in DMEM (ZR-75-1 and HeLa) or RPMI-1640 (H661 and MCF-7) medium with 10% fetal bovine serum (FBS) in a humidified atmosphere of 5% CO_2 at 37 °C. After the cells had been incubated in the logarithmic growth phase, samples with various concentrations of Dox were added for 24 and 72 h of co-culturing. At the end of the experiment, the MTT assay was conducted and the percentage of cell viability was calculated. Additionally, material cytotoxicities were measured using cells (5×10^3 cell mL^{-1}).

2.9. Method of internalization

To evaluate the utility of Dox-micelles as biomarkers, HeLa cells were seeded on coverslips for 1, 3 and 24 h and incubated at 25 and 37 °C under a 5% CO_2 atmosphere with ~1 μM Dox (as either free Dox or Dox-micelles). Next, each dish was washed with PBS (pH 7.4) for three times and loaded with LysoSensor™ Blue DND-167 for 30 min. Each dish was wash and treated with 1 mL of 4% paraformaldehyde solution for 10 min to fix the cells, and then mounted on a slide. Confocal laser scanning microscope (CLSM) was performed with a Leica TCS SP5 Confocal Spectral Microscope Imaging System using excitation wavelengths of 373, 488 and 675 nm and LP filters of 425, 590 and 695 nm to detect LysoSensor Blue DND-167, doxorubicin and Cy5.5, respectively.

2.10. Noninvasive imaging [26] and ex vivo fluorescence imaging [31]

To assess the *in vivo* distribution of micelles in tumor-bearing mice, HeLa cells (1×10^6 cells/0.1 mL) were transplanted subcutaneously to the abdomens of female BALB/c mice ($n = 3$); two weeks later, Cy5.5-modified Dox-micelles (1 mg doxorubicin/kg) were administered through the tail vein to the tumor-bearing mice (tumor size < 10 mm dia.). The mice were anesthetized by 1.5% isoflurane in 1:2 O_2/N_2 and optical images were acquired using an IVIS 100 imaging system (exposure time = 1 s) *via* the Cy5.5 filter channel before and after injection. Accumulation of Dox-micelles was calculated by dividing the NIR fluorescence intensity of the tumor (ROI1) by that of normal tissue (ROI2). Optical imaging was also performed on dissected tissues harvested immediately after the biodistribution studies. Harvested tissues were also frozen and embedded in OCT medium (MICROM). Frozen sections (20-μm thick) were cut using a microtome-cryostat (CM3050 S, Leica) and scanned immediately with an FLA-5000 PhosphorImager (Fujifilm) under the following conditions: 600 nm (red light) and 473 nm (blue light), 700 V, 65,536 tonal gradations and 25 μm resolution. All animal experiments were approved by the Animal Use Committee of the National Tsing Hua University.

2.11. In vivo antitumor activity [26,30]

The tumor model was established as described above. When the transplanted tumor volume reached approximately 50 mm^3 (7 days after inoculation), animals were randomly divided into two groups (experimental and control groups, six animals per group). Animals were treated i.v. *via* the tail vein at 3 different time points with an interval of 4 days (days 0, 4, and 8). Mice were injected with 0.2 mL of different formulations of doxorubicin solutions (Dox-Micelles and free doxorubicin at a dose of 5 mg/kg) or neat saline/empty micelles (negative control). Follow-up was performed for 43 days following the administration experiments were performed. During the course of the follow-up, tumor size was measured three times a week using a Vernier's caliper. Tumor volume was calculated as follows: $V=(ab^2)/2$ (where a and b indicate the major and minor axes of the tumor, respectively). Mice body weight (as an indirect indicator of general animal wellness) and clinical status were carefully recorded. To evaluate the antitumor activity, the relative tumor volume was calculated as the ratio of tumor volume on that day to its value at the start of therapy. To evaluate toxicity, we assessed mortality and relative body weight (calculated as the ratio of tumor volume on that day to its value at the start of therapy).

3. Results and discussion

3.1. Polymer characteristics

Micelles formed by mixing copolymers with distinctly different properties can be fine-tuned to meet the specific requirements of various applications [25,26,29,30,32], and both temperature- and pH-sensitive copolymers [29,32] have been used to form mixed micelles for drug delivery. Similarly, mixing a copolymer with a lower CMC prevents dissociation [25,29]. This can maintain the particles in the blood longer, increasing their uptake in peritumoral tissue by the EPR effect. Thus, using shell-forming block copolymers with significant differences to yield stable mixed micelles is highly desirable for drug delivery systems. mPEG-*b*-P(HPMA-Lac-*co*-His) had a composition of 0.9% PEG, 31.2% HPMA, 62.4% Lac, and 5.5% His, with weight average, number-average molecular weight and

polydispersity index (PDI) of 21553, 19244 and 1.12 by gel permeation chromatography and nuclear magnetic resonance measurements (In the Supporting Information). It has a CMC value of 1.25×10^{-2} mg/mL. Additionally, the CMC value of mPEG-PLA was 3.91×10^{-3} mg/mL. The heating rate is critical for micellar preparation within a narrow size based on temperature-sensitive polymers: Rapid heating favors the formation of small particles and thus was used to prepare mixed micelles [19–21]. DLS showed that a 75/25 mass ratio mPEG-*b*-P(HPMA-Lac-*co*-His) to mPEG-*b*-PLA produced micelles of optimal size and PDI (Fig. 2a). Polymer concentrations of 0.1, 0.5, 1, 1.5, 2.0 and 10 mg/mL produced empty mixed micelles of 15993.2, 96.7, 50.7, 51.9, 53.0 and 98.7 nm and PDIs of 0.87, 0.12, 0.09, 0.105, 0.118 and 0.273, respectively, presumably the result of the interpolymer aggregation that occurs at high polymer concentrations (Fig. 2b) [19].

3.2. Dual responsive micelles characterization

For drug delivery application of temperature-sensitive polymers, it is important to have possibilities to control the phase transition around body temperature. Poly(*N*-(2-hydroxypropyl) methacrylamide dilactate) are expected to form dual responsive micelles at 37 °C but gradually dissolve as the lactic acid side groups hydrolyze, releasing drugs loaded from the core into the tumor environment [19–24]. The temperature-sensitive of mPEG-*b*-P(HPMA-Lac), mPEG-*b*-P(HPMA-Lac-*co*-His) and mPEG-*b*-P(HPMA-Lac-*co*-His)/mPEG-*b*-PLA (75:25) was monitored by the changes in particle size and PDI as a function of temperature in Fig. 2c. The particle size significantly decreased as increasing temperature from 5.0 to 10.0 °C. PDI decrease gradually between 5.0 and 35.0 °C. On the other hand, the particle size of mPEG-*b*-PLA decreased as increasing temperature from 5.0 to 10.0 °C and 27.5–30.0 °C because the interior structure responded to temperature by altering microviscosity [33]. PDI decrease from 1.0 to 0.5 gradually between 17.5 and 27.5 °C (Fig. S4). This indicates that the temperature-dependent interior structure of mixed micelle relied on the portion of Poly(*N*-(2-hydroxypropyl) methacrylamide dilactate) and Poly(lactic acid) in hydrophobic core. Furthermore, mixed micelle showed a narrow size distribution in Fig. S4. To demonstrate the phase transition, the CP of mPEG-*b*-P(HPMA-Lac), mPEG-*b*-P(HPMA-Lac-*co*-His) and mPEG-*b*-P(HPMA-Lac-*co*-His)/mPEG-*b*-PLA (75:25) was determined to be around 5.5, 8.2 and 2.5 °C using a UV/Vis spectrophotometer at 542 nm (Fig. 2d). The CP of mPEG-*b*-P(HPMA-Lac) was similar temperature-sensitive of property to previously report [23]. The CP of mPEG-*b*-P(HPMA-Lac-*co*-His) showed a slight increase that may be attributed the histidine molecules disrupted the aggregation of HPMA-dilactate and caused sensitivity to temperature and pH because of protonation–deprotonation of the imidazole group [29]. The CP of mixture was lower than mPEG-*b*-P(HPMA-Lac-*co*-His) that might be caused by the altering microviscosity of mPEG-PLA and the lower CMC value. Equally important, empty mixed micelles had

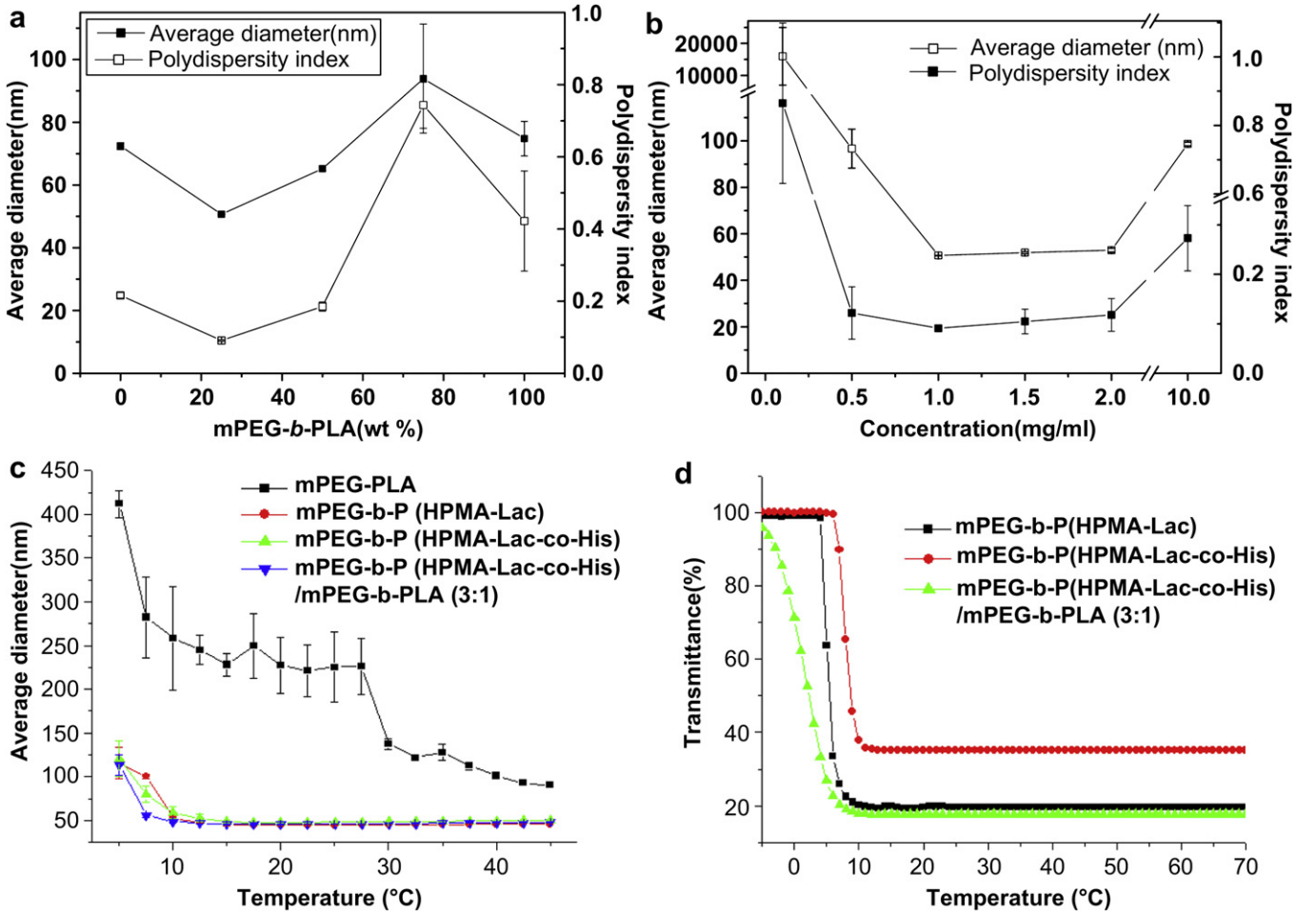

Fig. 2. Particle size and PDI influence by changing (a) composition ratio and (b) polymer concentrations. (c) Particle size of diblock copolymers in different temperature conditions by DLS analysis. (d) The cloud point of diblock copolymers.

a pH response < pH 7.0 at 37 °C and the pH-sensitive moiety (i.e., histidine) in the core–shell micelles were affected by lactic acid from the hydrophobic segment and environmental pH (Fig. 3a). The results demonstrate that the mixed micelles were efficient temperature- and pH-responsive carrier system with controlled instability based on the environment.

Dox-micelles were prepared through hot shock protocol. In our study, Dox-micelles were soluble and homogenous in PBS. At an initial Dox concentration of 8 mg/mL, the maximum amount of drug loaded in the micelle was 15.0 wt%, producing a slight increase in both the size and PDI of the micelle. However, at higher drug loading concentrations, the amount of diblock copolymer was insufficient to solubilize the hydrophobic drug, resulting in the formation of doxorubicin aggregates. At 1 h, the core–shell structure of Dox-micelle was apparent (Fig. 1c), and the size of the particles as measured by microscopy was similar to that determined by DLS (Fig. 1b). Dox-micelle of optimal size (50.7 nm) and PDI (0.12) had a slightly negative zeta potential (−1.8 ± 0.7 mV) resulting from the outer shell of mPEG [28]. After 12 h, Particle size progressively increased from 50.7 to 72.7 nm in buffer solution (pH 7.4). On the other hand, particle size of mPEG-*b*-P(HPMA-Lac-*co*-His) micelles gradually increased, but had broader size distribution than mixed micelle after 3 h (Fig. S5). The results suggested mixed micelle with low CMC copolymer could prevent dissociation of any copolymer from micelle and improved the stability [25,29]. Although, blood half-life of the 60 nm pegylated nanoparticles was 16.5 h, 100 nm particles carried the greatest total mass to the tumor owing to their larger volume [11]. Small particles (≤60 nm) diffused throughout blood vasculature. Motivated by this rationale, we suggest the dual-responsive drug carriers could stay in tumor extracellular matrix (ECM) because the particle size increasing gradually at near neutral pH.

3.3. Miscibility of two copolymers in micelles

The miscibility of two types of diblock copolymers in a mixed micelle system was confirmed by a DSC analysis. DSC not only was used to demonstrate the miscibility of the mixed micelles, but also be performed to further study the thermal properties of diblock copolymers. For confirm the miscibility of the mixed micelles, the mixture of single-component micelles was the unmixed reference. Fig. 4a and b plots the first and second DSC traces of mPEG-*b*-PLA micelles, mPEG-*b*-P(HPMA-Lac-*co*-His) micelles, mixed micelles and the mixture of mPEG-*b*-PLA micelles and mPEG-*b*-P(HPMA-Lac-*co*-His) micelles in a 1:1 weight. The first heating trace shows an endothermic peak corresponding to the fusion of the crystallites in the samples; the melting enthalpy corresponds to the total amount of PEG in the samples [34]. Compared to the other heating trace, the melting endotherm of mixture appears unclear two peaks, indicating that a phase separation occurred between two kinds of micelles. On the other hand, the melting endotherm of mixed micelles was a signal peak and similar to the heating trace of mPEG-*b*-P(HPMA-Lac-*co*-His) micelles. The second heating trace shows the weak step of mPEG-*b*-PLA micelles, mPEG-*b*-P(HPMA-

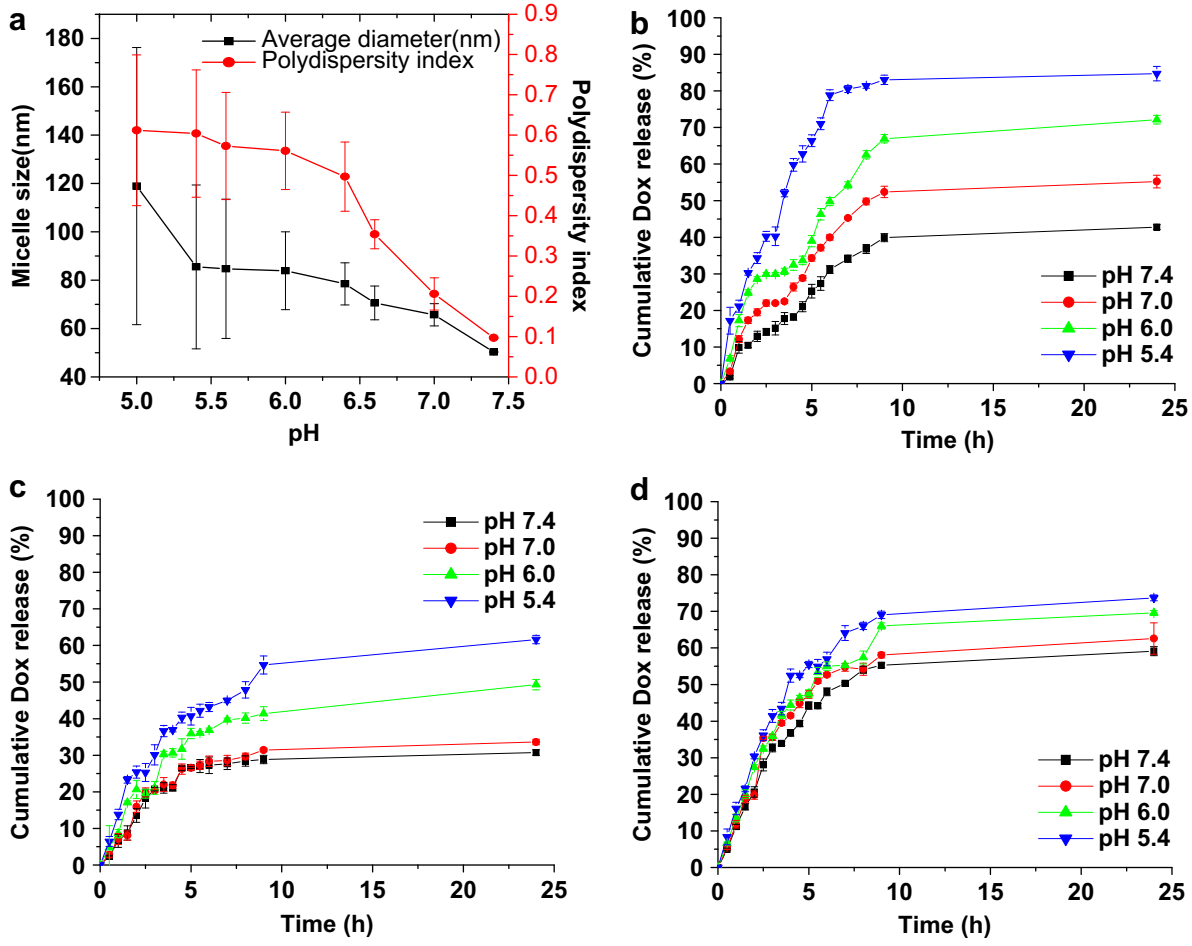

Fig. 3. (a) The size and PDI of mixed micelle in different pH of PBS buffers by DLS analysis. Effects of pH on doxorubicin release from dual responsive micelle *in vitro* at 37 °C (b) and 25 °C (c). (d) Effect of pH on doxorubicin release from mPEG-*b*-P(HPMA-Lac) micelle *in vitro* at 37 °C. ($n = 3$).

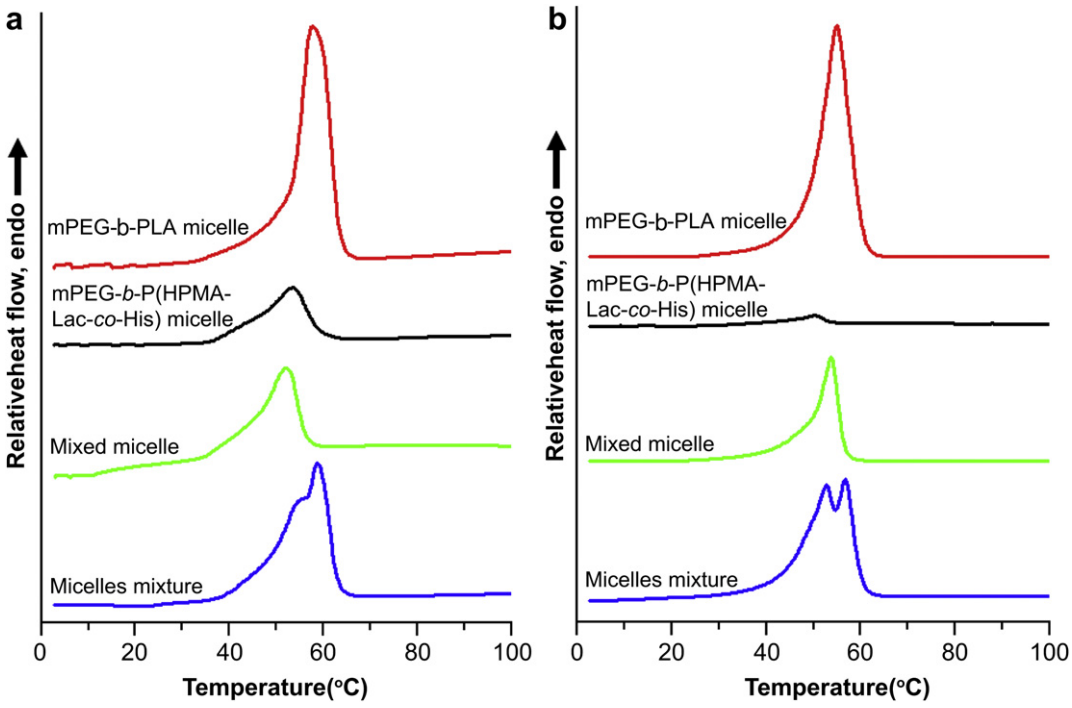

Fig. 4. The first run (a) and second run (b) of DSC thermograms of mPEG-b-PLA micelle, mPEG-*b*-P(HPMA-Lac-*co*-His) micelle, mixed micelle and micelle mixture with equal weight ratio of mPEG-*b*-P(HPMA-Lac-*co*-His) and mPEG-b-PLA micelle.

Lac-*co*-His) micelles and mixed micelles in the specific heat observed at 34.1 and 22.7, 24.7 °C, respectively. The glass transition temperature of poly(lactic acid) and ranged from 20 to 50 °C as the degree of polymerization varied [35]. The glass transition temperature of mPEG-*b*-PLA micelles was similar with previous report [29]. The glass transition temperature could be ascribed to HPMA, PLA and lactate. The glass transition temperature of the mixed micelles was between to glass transition temperature of mPEG-*b*-P(HPMA-Lac-*co*-His) and mPEG-*b*-PLA micelles, explaining the miscibility of the mixed micelles. The glass transition temperature of the mixture of mPEG-*b*-PLA micelles and mPEG-*b*-P(HPMA-Lac-*co*-His) micelles in a 1:1 weight ratio did not exhibit secondary transition but exhibited two endotherm transitions at around 52.3 and 56.5 °C associated with mPEG, demonstrating the immiscibility of the single-component micelles. Moreover, the narrow size distribution polydispersity of the micelles (Fig. S4) infers the co-micellization of the two copolymers which were miscibility. The results indicate that two copolymers were completely miscible in mixed micelles with homogenous cores where PLA and P(HPMA-Lac-*co*-His) coexist.

3.4. pH-dependent drug release

As mentioned above, dual responsive micelles had the temperature- and pH- response and encapsulated doxorubicin stably. To illustrate dual responsive drug release profile, the micelles were performed under physiological condition (pH 7.4), endosomal (pH 6.6 and 6.0) and lysosomal (pH 5.4) environment at room and body temperature. The drug release profile of mixed micelles at 37 °C was shown in Fig. 3b. Mixed micelles released doxorubicin in an initial burst (~15%) at pH 7.4. At pHs of 6.0 and 6.6, 38.9 and 34.3% of the drug was released within 5 h, respectively. In contrast, at pH 5.4, drug release occurred rapidly (66.4%) during the initial 5 h. The pH-dependent release profiles had the same trend as other pH-responsive micelles with the pH-sensitive moiety [14,15,36]. However, the drug release profiles of mixed micelles were significantly different between room and body temperature. The drug release profile of mixed micelles at 25 °C was shown in Fig. 3c, pHs of 6.0, 6.6 and 7.4, 35.9, 26.6 and 26.6% of the drug was released within 5 h, respectively. At either temperature, release speed at pH 5.4 was higher than at pH 7.4. From comparison of Fig. 3b and c, a higher temperature was found to be helpful for drug release because the hydrolysis rate of lactic acid side groups increased at higher temperature [37], which makes drug movement within the hydrophobic core easier. The release profile of mPEG-*b*-P(HPMA-Lac) micelles at 37 °C was shown in Fig. 3d, 44.3% and 59.7% of doxorubicin was released in pH 7.4 buffer solutions after 5 h and 24 h, respectively. This result was similar to the release profile of mPEG-*b*-P(HPMA-Lac) micelles encapsulating paclitaxel under the same condition [19]. At pH 7.4 and at 37 °C, degradation half-lives of poly(2-hydroxyethyl) methacrylate-dilactate) and poly(2-hydroxyethyl)methacrylate-monolactate) are 15 and 87 h, respectively [38]. This behavior has been ascribed to the conversion of the hydrophobic poly(2-hydroxyethyl)methacrylate-dilactate) core to the more hydrophilic poly(2-hydroxyethyl)methacrylate-monolactate) and finally to water soluble p((2-hydroxyethyl)methacrylate) [38,39]. As a result of hydrolysis of the lactic acid side groups, mPEG-*b*-P(HPMA-Lac) yielded water soluble mPEG-*b*-pHPMA block copolymer chains gradually. Release speeds at pH 5.4, 6.6 and 7.0 were slight higher than that at pH 7.4, could be ascribed to hydrolysis rate of lactic acid side groups increased under acidic environment [40]. Notably, the release behavior of dual responsive micelles were more pH-dependent than mPEG-*b*-P(HPMA-Lac) micelles.

The temperature- and pH-dependent of dual responsive micelles likely results from a number of factors: hydrolysis of lactic acid side groups, conferral of pH-dependent amphoteric properties from the electron pair on the unsaturated nitrogen of histidine, triggering of the imidazole ring by the lactic acid of the hydrophobic core. Consequently, temperature at 37 °C and pHs below 7.4 triggered doxorubicin release from the micelles. This is significant because the

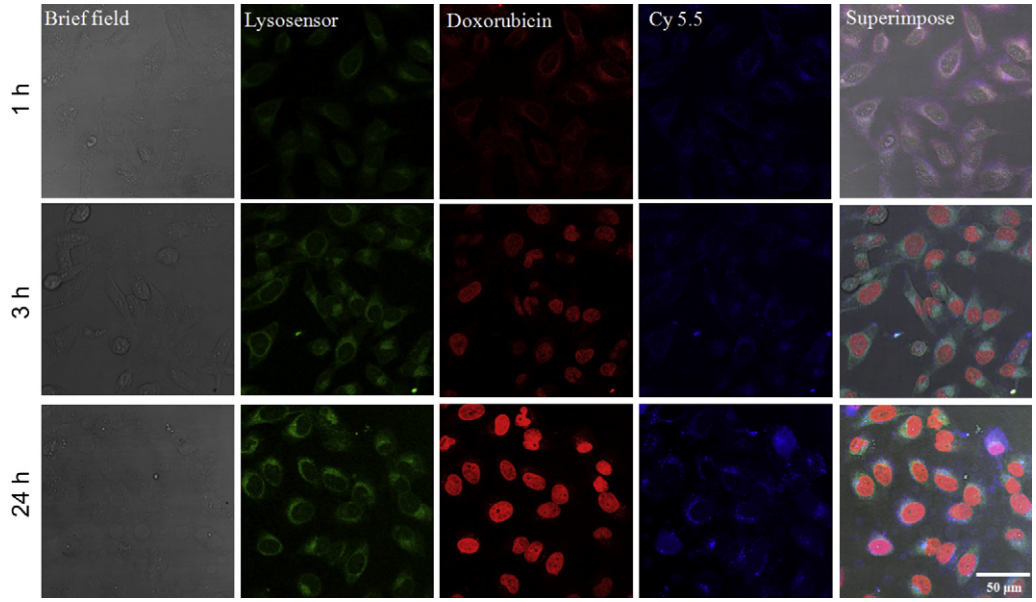

Fig. 5. Confocal images of HeLa cells incubated with Cy5.5 tagged Dox-micelle at 37 °C after 1, 3 and 24 h for evaluating drug in intracellular drug delivery.

drug carriers aggregate and accumulate at tumor sites with slight lower extracellular pHs [13] and body temperature; this can enhance the therapeutic effects of passively targeted.

3.5. Micelles and drug uptake evaluation

Confocal microscopy was applied to observe the intracellular distribution of internalized carriers and doxorubicin. To determine the cellular distribution more precisely, we performed one fluorescence – labeling experiments and visualized red fluorescence from doxorubicin, blue fluorescence from Cy5.5-tagged micelles and green fluorescence from LysoSensor Blue DND-167, dye that is selective for acidic lysosomes (or endosomes), respectively. As monitored by CLSM, HeLa cells incubated with Cy5.5-tagged Dox-micelles at 37 °C for 1 h showed blue and red fluorescence in the cytoplasm (Fig. 5). This is consistent with observations that the triggering mechanisms for most particulate carriers occur in the endosome and release the drugs into the cytoplasm. Indeed, pH drops significantly from 7.2 to 7.4 to 5.0–6.5 in the endosomes, and to ~pH 4.5 in primary and secondary lysosomes [2,3] by being observed green fluorescence. After 3 and 24 h, released doxorubicin was more and more apparent with increasing time in the nuclei, whereas the Cy5.5-tagged micelles remained localized mostly in the cytoplasm. This provides strong evidence that HeLa cells take up the micelles and that the drug is released intracellularly and finally diffusion into the nuclei. To compare the intracellular distribution at 25 °C with that at 37 °C, HeLa cells incubated with Cy5.5-tagged Dox-micelles at 25 °C for 1 h (Fig. S6) showed a similar result to Fig. 5. Notably, red fluorescence was apparent remained localized

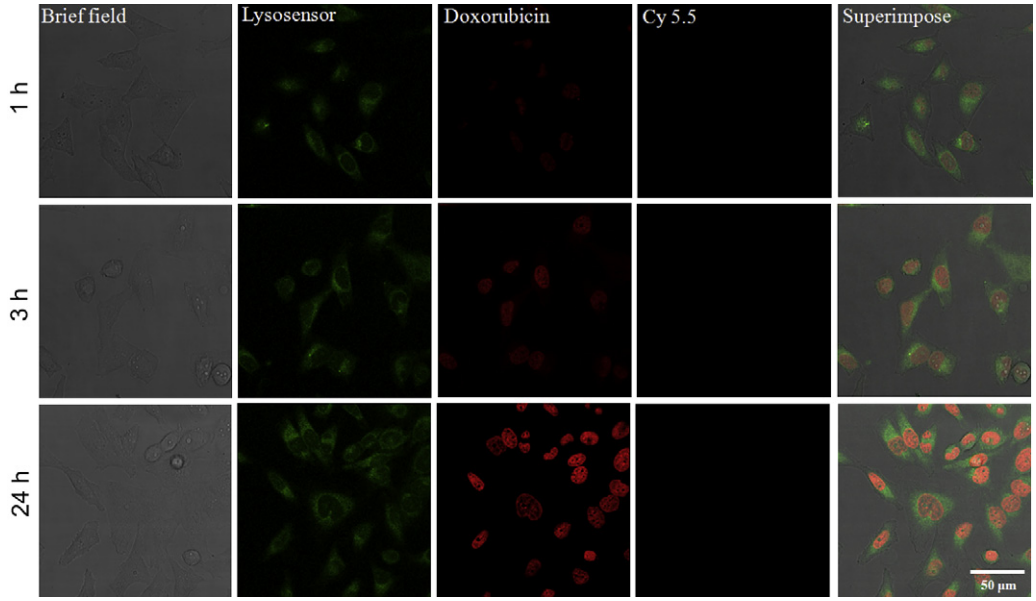

Fig. 6. Confocal images of HeLa cells incubated with doxorubicin at 37 °C after 1, 3 and 24 h for evaluating drug in intracellular drug delivery.

mostly in the cytoplasm after 3h. The results demonstrated that a higher temperature was helpful for intracellular drug release. After 24 h, released doxorubicin was apparent in the nuclei. On the other hand, HeLa cells incubated with free doxorubicin for 1 h showed red fluorescence in the nuclei (Fig. 6). Free doxorubicin was passive diffusion into HeLa cells and immediate accumulation in the nuclei. After 3 and 24 h, weaker red fluorescence accumulation into the nuclei compared with encapsulated doxorubicin than treated with Dox-micelles. Despite delivery by different route, released doxorubicin from Cy5.5-labeled micelles was more effective accumulation into the nuclei, which is similar to other particulate [41,42].

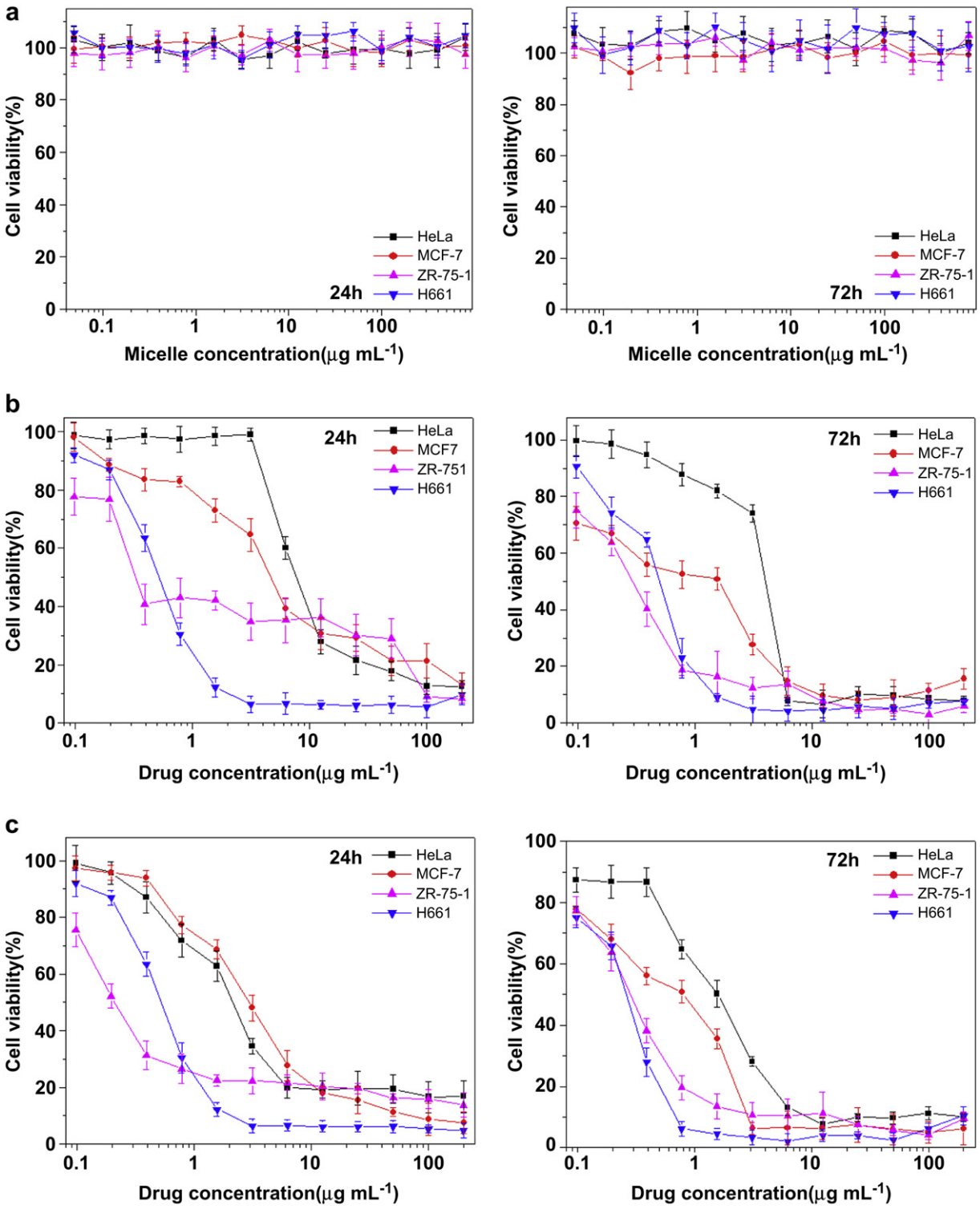

Fig. 7. Cytotoxicity of (a) empty micelle (b) doxorubicin and (c) Dox-micelle on cells after 24 (left) and 72 h (right) of incubation *in vitro*. Data are the means and standard deviations of nine independent experiments.

Table 1
IC_{50} values of free doxorubicin and Dox-loaded micelle for cancer cells.

Cell lines	IC50 (μg/mL)			
	Dox		Dox-Micelle	
	24 h	72 h	24 h	72 h
HeLa	8.22	4.26	2.97	1.58
MCF-7	4.93	1.95	2.27	0.83
ZR-75-1	0.55	0.53	0.55	0.30
H661	0.34	0.31	0.20	0.28

3.6. Cytotoxicities

To compare cytotoxic activity of loaded and free drug, HeLa, ZR-75-1, MCF-7 and H661 cells were exposed to a series of equivalent concentrations of free doxorubicin or doxorubicin encapsulated in micelles for 24 and 72 h, and the percentage of viable cells was quantified using the methylthiazoletetrazolium method. Empty micelles displayed no significant cytotoxicity toward any of the tumor cell lines tested after 24 or 72 h *in vitro*, demonstrating they are non-cytotoxic (Fig. 7a). In contrast, the viability of all cells depended on the doxorubicin concentration (Fig. 7b and c). Table 1 presents inhibition concentration (IC_{50}) of free drug and Dox-micelles. Doxorubicin and Dox-micelles were all more cytotoxic, and at lower concentrations, after 72 h of incubation than after 24 h. Notably, Dox-micelles were more cytotoxic than free doxorubicin. The results were suggested not only Dox-micelles were endocytosis by cells with sight negative zeta potential surface, but also brusted with higher drug concentration at pH 5.4 and 37 °C similar to acidic endosomal compartment. As verified by the CLSM analysis, Dox-micelles can release drug into the cell nuclei effectively with a more controlled manner initially in the acidic endocytic compartments. These results indicate that the encapsulated doxorubicin from dual responsive micelles plays an important role in the enhancement of cytotoxic activity.

3.7. In vivo biodistribution

Despite excellent physical properties *in vitro*, many nanoparticles prove unsatisfactory as drug carriers *in vivo* because of their instability, undesirable biodistribution, and low targetability. To determine drug delivery by the carriers affected the targeted tumor *in vivo*, we treated Balb/c nude mice bearing human cervical tumors with one injection of Cy5.5-tagged Dox-micelles. Live animal imaging showed that fluorescence intensity was stronger at the tumor site than at normal tissues, suggesting that the mixed micelles were targeting the tumors preferentially by passive tumor targeting (EPR effect) (Fig. 8a). Furthermore, the relative fluorescence intensity in tumors increased gradually: 1, 3 and 24 h after intravenous injection, accumulation of the Dox-micelles was 1.27 ± 0.148, 1.42 ± 0.026 and 1.83 ± 0.221, respectively. This result demonstrated that the particles could be delivery by tumor selective targeting, and not diffuse throughout the tumor matrix at 24 h after intravenous injection. Doxorubicin is highly toxic to both endothelial cells and cardiomyocytes [43,44], which accounts for some of the adverse side effects associated with its systemic administration. However, fluorescence intensity images of tissues dissected 24 h after injection showed strong accumulation in tumors but not in other tissues (Fig. 8b). The low intensities in the liver and spleen suggest that the particle increased size in the tumor interstitial space, and the particles could not diffuse throughout the tumor matrix. Moreover, micelles incorporating a PEG shell avoided recognition by monocytes and entrapment by hepatic sinusoidal capillaries [27,28]. To illustrate drug biodistribution, phosphorimaging of sectioned tissues was visualized red and blue fluorescence from doxorubicin and Cy5.5-tagged micelles [30,31], respectively. Similarly, the images showed a significant and nearly overlapping accumulation of mixed micelles and doxorubicin in tumors (Fig. 9). Doxorubicin and Cy5.5-tagged micelles fluorescence could not notable observe from other normal tissue. The dual-responsive drug carriers not only deliver micelles selectively to the tumor site, but also accumulate and release anticancer drug in pathological tissue.

3.8. In vivo antitumor activity

To examine *in vivo* antitumor efficacy of dual responsive micelles, Balb-c/nude mice bearing human cervical tumors were treated with saline, empty micelles, doxorubicin or Dox-micelles. All the treatment modalities were administered by intravenous injection with a frequency of four times at a 4 day interval when the tumors reached a volume of 0.5 cm^3. The growth of subcutaneously-implanted tumors was assessed over a 43-day time frame. Tumor

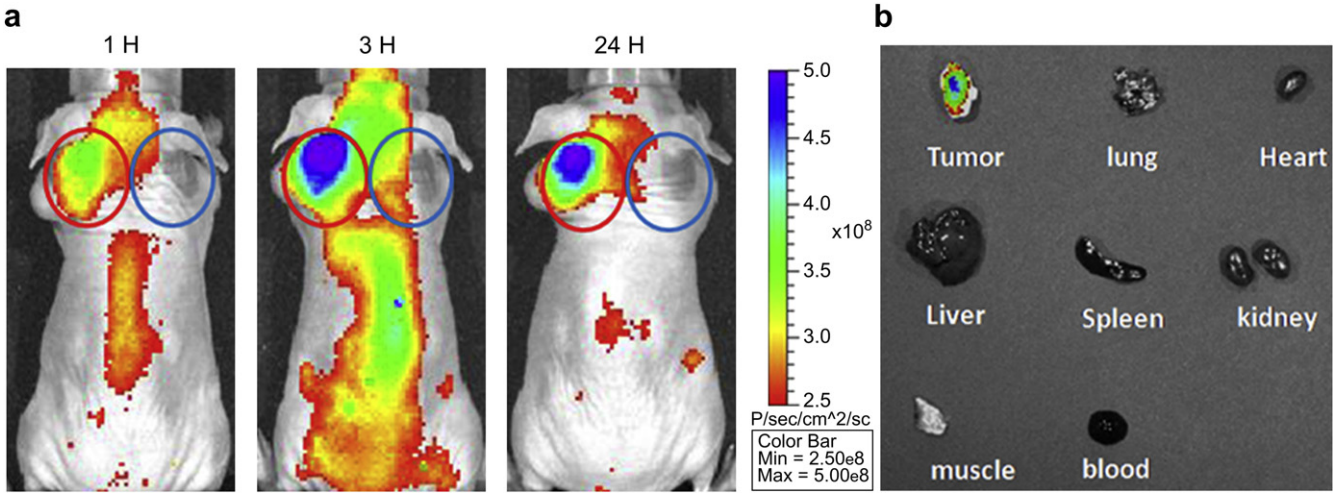

Fig. 8. (a) Optical fluorescence imaging *in vivo* of HeLa tumors xenografted into nude mice and treated with Cy5.5-Dox-micelle. The red (ROI1) and blue (ROI2) cycles indicate the locations of tumor and normal tissues, respectively. (b) Photoimaging of organs and tumors harvested 24 h posttreatment with 2 mg/kg of Dox-micelle. Colors indicate relative fluorescence. (For interpretation of the references to colour in this figure legend, the reader is referred to the web version of this article.)

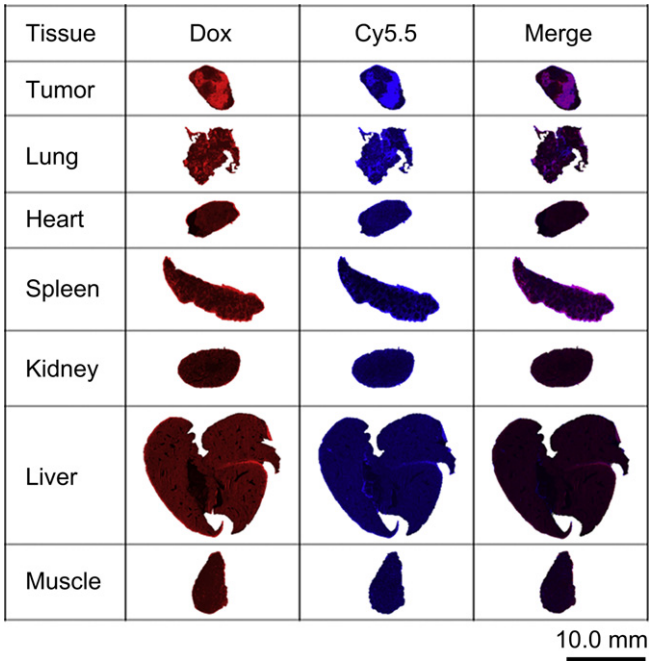

Fig. 9. Phosphorimages of mouse organs harvested 24 h after iv injection of micelle.

volumes of the untreated (control) and treated mice with free doxorubicin increased very rapidly (ca. 16.7- and 12.0-fold increase, respectively) (Fig. 10a). In addition, tumor volumes of the empty micelles and saline showed the same trend as control. Empty micelles displayed no antitumor activity and were non-effect on the treatment. Mice treated with Dox-micelles showed slow increase (5.5-fold) after 43 days. The clearly results suggest that Dox-micelles showed a considerably higher antitumor activity compared with free doxorubicin. Administration of doxorubicin is associated with some acute side effects (including myelosuppression and gastrointestinal toxicity) as well as a cumulative dose-limiting cardiotoxicity [43–45]. Many reports *in vivo* experiments indicate a well-designed polymeric carrier to ameliorate both acute and chronic toxic side effects of doxorubicin [26,30,45]. Body weight loss is one of indicators to evaluate doxorubicin-induced toxicity. Mice treated with free doxorubicin at a concentration of 5 mg/kg exhibited a 13% decrease of body weight within 8 days (3 injections), and appeared to be weak after treatment (Fig. 10b). Treatment with Dox-micelles resulted in a minimal weight loss (approximately 1%), suggesting that this drug carrier could phenomenal reduce doxorubicin toxicity to normal tissues. Saline and empty micelles showed the mice gained weight because the tumor volumes increased rapidly. This better *in vivo* antitumor activity could be attributed to selective targeting, tumor-specific accumulation and effective release from controllable increasing particle size.

To our knowledge, this study demonstrated biodegradable dual responsive particles could enhance permeation through the tumor site. Most peripheral human tumors grown subcutaneously exhibited a characteristic pore cutoff size ranging from 200 to 600 nm [46]. Accordingly, particle size is one of critical factor to design of tumor targeting nanoparticles. The internalization of Herceptin-gold nanoparticles complex was highly dependent on size, with the most efficient cell uptake occurring within the 40–50 nm size range [8]. Pegylated gold nanoparticles were demonstrated that 60–100 nm particle would provide excellent blood pharmacokinetics and tumor accumulation and could be used to localize leaky vasculature [11]. Although the size and behavior of polymeric micelles may be quite distinct from that of colloidal metal particles, the example offer an ideal size range for drug delivery system. After intravenous injection, polymeric micelles caused selective disintegration and enlargement of the tumor blood vessel bed [5]. The inherent pore size of the tumor vessel wall is larger and larger. These studies provided strong evidence that small particles (≤60 nm) are inappropriate for passive accumulation in the tumor compartment because of rapidly diffusion of interstitial space permeation. The particle size-dependent permeation of the tumor site reveals the phenomenon that pore cutoff size of the tumor vessel wall can explain the extravasation characteristics of the dual responsive micelles.

The results of this study indicate that biodegradable dual responsive particles exhibit a specific targeting efficiency and an excellent antitumor activity. We suggest several reasons may explain these substantial findings. Fundamentally, the micelles are hydrophilic, nonimmunogenic, and non-toxic, the components of which have been evaluated clinically or *in vivo*. Dual responsive

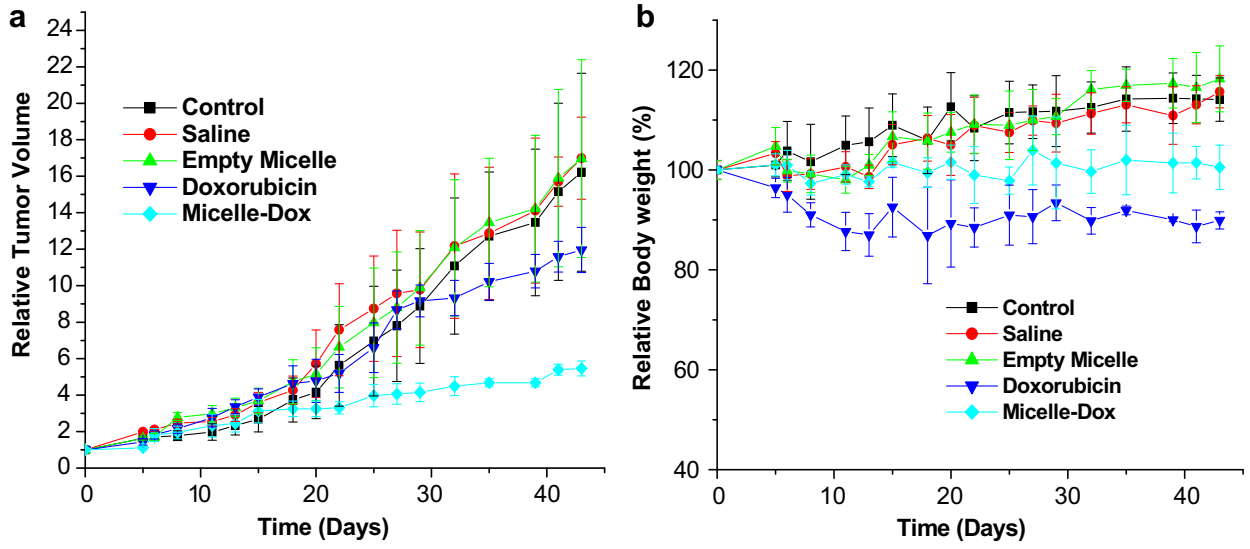

Fig. 10. (a) *In vivo* anticancer efficacy and (b) body weight changes in Balb-c/nude mice bearing HeLa tumors after intravenous administration of free doxorubicin, micelle-Dox, empty micelle, saline and controlled.

micelles have a suitable and narrow particle size distribution originally. After intravenous injection, the mPEG surface brush layer with stealth behavior used to be long-circulating particles, which reduces the adsorption of reticuloendothelial system (RES) causes to the micelle surface and diminishes the rate of clearance of micelle by cells of the monophagocytic system (MPS) [27,28]. Subsequently, dual responsive micelles increased size to restrict particle extravasation while increasing accumulation at tumor sites. Dual responsive micelles were destroyed by the change in intracellular pH/body temperature and release the anticancer drug rapidly. Thus, released drug from dual responsive micelle was more efficient accumulation into the nuclei and enhanced the cytotoxic activity. The *in vivo* behavior and tumor targeting capacity of dual responsive micelle appears to be ideally suited to the design of tumor targeting carriers as it allows for tumor accumulation, permeation and therapy.

4. Conclusions

In summary, we have developed a mixed micelles temperature- and pH-responsive to trigger drug release and enhance passive targeting. The slight acidic environment and body temperature found near tumors results in the specific release of drugs from the mixed micelles. The micelles delivered doxorubicin efficiently to the nuclei of cells *in vitro*. The carrier also delivered drugs specifically to tumors *in vivo* with restrictive particle extravasation. The particles' properties could prolong circulation time and reduce side effects, making it therapeutically appealing. Furthermore, the use of the Cy5.5-tagged and noninvasive imaging techniques make it delineate subcutaneous tumors from the surrounding tissue. We anticipate the high effectiveness and non-cytotoxic of dual responsive micelle system provides a strategy for a promoting further assess the applicability of stimuli-responsive nanoparticles for cancer treatment.

Acknowledgment

This work was supported partly by a grant from the Taiwan Chang Gung Memorial Hospital, University of Tsing-Hua Joint Research Program (NO. 100N2732E1, CMRPG390071 and CMRPG3A0041) and partly by another grant from the National Science Council of the Republic of China (99- and 100-2120-M-033-001-). TTY biopharm Co. Ltd. (Taiwan) is appreciated for kindly providing the doxorubicin hydrochloride. We thank the excellent technical assistance of Technology Commons, College of Life Science, NTU (Taiwan) with CLSM and TEM.

Appendix A. Supplementary data

Supplementary data related to this article can be found online at doi:10.1016/j.biomaterials.2012.02.059.

References

[1] Wiradharma N, Zhang Y, Venkataraman S, Hedrick JL, Yang YY. Self-assembled polymer nanostructures for delivery of anticancer therapeutics. Nano Today 2009;4:302–17.
[2] Davis ME, Chen Z, Shin DM. Nanoparticle therapeutics: an emerging treatment modality for cancer. Nat Rev Drug Discov 2008;7:771–82.
[3] Haag R, Kratz F. Polymer therapeutics: concepts and applications. Angew Chem Int Ed Engl 2006;45:1198–215.
[4] Maeda H, Wu J, Sawa T, Matsumura Y, Hori K. Tumor vascular permeability and the EPR effect in macromolecular therapeutics: a review. J Control Release 2000;65:271–84.
[5] Maeda H. Tumor-selective delivery of macromolecular drugs via the EPR effect: background and future prospects. Bioconjug Chem 2010;21:797–802.
[6] Pirollo KF, Chang EH. Does a targeting ligand influence nanoparticle tumor localization or uptake? Trends Biotechnol 2008;26:552–8.
[7] Jiang W, Kim Betty YS, Rutka JT, Chan Warren CW. Nanoparticle-mediated cellular response is size-dependent. Nat Nanotechnol 2008;3:145–50.
[8] Geng Y, Dalhaimer P, Cai S, Tsai R, Tewari M, Minko T, et al. Shape effects of filaments versus spherical particles in flow and drug delivery. Nat Nanotechnol 2007;2:249–55.
[9] Lundqvist M, Stigler J, Elia G, Lynch I, Cedervall T, Dawson KA. Nanoparticle size and surface properties determine the protein corona with possible implications for biological impacts. Proc Natl Acad Sci USA 2008;105:14265–70.
[10] Larsen EKU, Nielsen T, Wittenborn T, Birkedal H, Vorup-Jensen T, Jakobsen MH, et al. Size-dependent accumulation of PEGylated silane-coated magnetic iron oxide nanoparticles in murine tumors. ACS Nano 2009;3:1947–51.
[11] Perrault SD, Walkey C, Jennings T, Fischer HC, Chan WCW. Mediating tumor targeting efficiency of nanoparticles through design. Nano Lett 2009;9:1909–15.
[12] Stefanadis C, Chrysochoou C, Markou D, Petraki K, Panagiotakos DB, Fasoulakis C, et al. Increased temperature of malignant urinary bladder tumors in vivo: the application of a new method based on a catheter technique. J Clin Oncol 2001;19:676–81.
[13] Tannock IF, Rotin D. Acid pH in tumors and its potential for therapeutic exploitation. Cancer Res 1989;49:4373–84.
[14] Soppimath KS, Tan DCW, Yang YY. pH-triggered thermally responsive polymer core-shell nanoparticles for drug delivery. Adv Mater 2005;17:318–23.
[15] Zhang L, Guo R, Yang M, Jiang X, Liu B. Thermo and pH dual-responsive nanoparticles for anti-cancer drug delivery. Adv Mater 2007;19:2988–92.
[16] Isojima T, Lattuada M, Vander Sande JB, Hatton TA. Reversible clustering of pH- and temperature-responsive Janus magnetic nanoparticles. ACS Nano 2008;2:1799–806.
[17] Chung JE, Yokoyama M, Aoyagi T, Sakurai Y, Okano T. Effect of molecular architecture of hydrophobically modified poly(N-isopropylacrylamide) on the formation of thermoresponsive core-shell micellar drug carriers. J Control Release 1998;53:119–30.
[18] Takakura Y, Hashida M. Macromolecular drug carrier systems in cancer chemotherapy: macromolecular prodrugs. Crit Rev Oncol Hematol 1995;18:207–31.
[19] Soga O, van Nostrum CF, Fens M, Rijcken CJF, Schiffelers RM, Storm G, et al. Thermosensitive and biodegradable polymeric micelles for paclitaxel delivery. J Control Release 2005;103:341–53.
[20] Rijcken CJF, Hofman J-W, van Zeeland F, Hennink WE, van Nostrum CF. Photosensitiser-loaded biodegradable polymeric micelles: preparation, characterisation and in vitro PDT efficacy. J Control Release 2007;124:144–53.
[21] Talelli M, Rijcken CJF, Lammers T, Seevinck PR, Storm G, van Nostrum CF, et al. Superparamagnetic iron oxide nanoparticles encapsulated in biodegradable thermosensitive polymeric micelles: toward a targeted nanomedicine suitable for image-guided drug delivery. Langmuir 2009;25:2060–7.
[22] Soga O, van Nostrum CF, Hennink WE. Poly(N-(2-hydroxypropyl) methacrylamide mono/di lactate): a new class of biodegradable polymers with tuneable thermosensitivity. Biomacromolecules 2004;5:818–21.
[23] Soga O, van Nostrum CF, Ramzi A, Visser T, Soulimani F, Frederik PM, et al. Physicochemical characterization of degradable thermosensitive polymeric micelles. Langmuir 2004;20:9388–95.
[24] van Nostrum CF, Veldhuis TFJ, Bos GW, Hennink WE. Tuning the degradation rate of poly(2-hydroxypropyl methacrylamide)-graft-oligo(lactic acid) stereocomplex hydrogels. Macromolecules 2004;37:2113–8.
[25] Lee ES, Na K, Bae YH. Super pH-Sensitive multifunctional polymeric micelle. Nano Lett 2005;5:325–9.
[26] Tsai HC, Chang WH, Lo CL, Tsai CH, Chang CH, Ou TW, et al. Graft and diblock copolymer multifunctional micelles for cancer chemotherapy and imaging. Biomaterials 2010;31:2293–301.
[27] Papisov MI. Theoretical considerations of RES-avoiding liposomes: molecular mechanics and chemistry of liposome interactions. Adv Drug Deliv Rev 1998;32:119–38.
[28] Gref R, Domb A, Quellec P, Blunk T, Müller RH, Verbavatz JM, et al. The controlled intravenous delivery of drugs using PEG-coated sterically stabilized nanospheres. Adv Drug Deliv Rev 1995;16:215–33.
[29] Lo CL, Lin SJ, Tsai HC, Chan WH, Tsai CH, Cheng CHD, et al. Mixed micelle systems formed from critical micelle concentration and temperature-sensitive diblock copolymers for doxorubicin delivery. Biomaterials 2009;30:3961–70.
[30] Lu PL, Chen YC, Ou TW, Chen HH, Tsai HC, Wen CJ, et al. Multifunctional hollow nanoparticles based on graft-diblock copolymers for doxorubicin delivery. Biomaterials 2011;32:2213–21.
[31] Knol RJJ, de Bruin K, de Jong J, van Eck-Smit BLF, Booij J. In vitro and ex vivo storage phosphor imaging of short-living radioisotopes. J Neurosci Methods 2008;168:341–57.
[32] Lo CL, Lin KM, Huang CK, Hsiue GH. Self-assembly of a micelle structure from graft and diblock copolymers: an example of overcoming the limitations of polyions in drug delivery. Adv Funct Mater 2006;16:2309–16.
[33] Na K, Lee KH, Lee DH, Bae YH. Biodegradable thermo-sensitive nanoparticles from poly(l-lactic acid)/poly(ethylene glycol) alternating multi-block copolymer for potential anti-cancer drug carrier. Eur J Pharm Sci 2006;27:115–22.
[34] Akiba I, Ohba Y, Akiyama S. Phase structure in blends of poly(ethylene glycol) and poly(styrene-co-methacrylic acid). Macromolecules 1999;32:1175–9.
[35] Omelczuk MO, McGinity JW. The influence of polymer glass transition temperature and molecular weight on drug release from tablets containing poly (DL-lactic acid). Pharm Res 1992;9:26–32.

[36] Kim D, Lee ES, Oh KT, Gao ZG, Bae YH. Doxorubicin-loaded polymeric micelle overcomes multidrug resistance of cancer by double-targeting folate receptor and early endosomal pH. Small 2008;4:2043–50.
[37] Coffin M, McGinity J. Biodegradable pseudolatexes: the chemical stability of poly (D, L-lactide) and poly (ε-caprolactone) nanoparticles in aqueous media. Pharm Res 1992;9:200–5.
[38] Rijcken CJF, Veldhuis TFJ, Ramzi A, Meeldijk JD, van Nostrum CF, Hennink WE. Novel fast degradable thermosensitive polymeric micelles based on PEG-block-poly(N-(2-hydroxyethyl)methacrylamide-oligolactates). Biomacromolecules 2005;6:2343–51.
[39] Neradovic D, van Steenbergen MJ, Vansteelant L, Meijer YJ, van Nostrum CF, Hennink WE. Degradation mechanism and kinetics of thermosensitive polyacrylamides containing lactic acid side chains. Macromolecules 2003;36:7491–8.
[40] de Jong SJ, Arias ER, Rijkers DTS, van Nostrum CF, Kettenes-van den Bosch JJ, Hennink WE. New insights into the hydrolytic degradation of poly(lactic acid): participation of the alcohol terminus. Polymer 2001;42:2795–802.
[41] Goren D, Horowitz AT, Tzemach D, Tarshish M, Zalipsky S, Gabizon A. Nuclear delivery of doxorubicin via folate-targeted liposomes with bypass of multidrug-resistance efflux pump. Clin Cancer Res 2000;6:1949–57.
[42] Li Y-L, Zhu L, Liu Z, Cheng R, Meng F, Cui J-H, et al. Reversibly stabilized multifunctional dextran nanoparticles efficiently deliver doxorubicin into the nuclei of cancer cells. Angew Chem Int Ed Engl 2009;48:9914–8.
[43] Hamed S, Barshack I, Luboshits G, Wexler D, Deutsch V, Keren G, et al. Erythropoietin improves myocardial performance in doxorubicin-induced cardiomyopathy. Eur Heart J 2006;27:1876–83.
[44] Wang S, Konorev EA, Kotamraju S, Joseph J, Kalivendi S, Kalyanaraman B. Doxorubicin induces apoptosis in normal and tumor cells via distinctly different mechanisms. J Biol Chem 2004;279:25535–43.
[45] Mayer LD, Tai LCL, Ko DSC, Masin D, Ginsberg RS, Cullis PR, et al. Influence of vesicle size, lipid composition, and drug-to-lipid ratio on the biological activity of liposomal doxorubicin in mice. Cancer Res 1989;49:5922–30.
[46] Yuan F, Dellian M, Fukumura D, Leunig M, Berk DA, Torchilin VP, et al. Vascular permeability in a human tumor xenograft: molecular size dependence and cutoff size. Cancer Res 1995;55:3752–6.